Alzheimer's & Dementia: Diagnosis, Assessment & Disease Monitoring 9 (2017) 1-9

Neuroimaging

Longitudinal changes in amyloid positron emission tomography and volumetric magnetic resonance imaging in the nondemented Down syndrome population

Patrick J. Lao[a,*], Ben L. Handen[b], Tobey J. Betthauser[a], Iulia Mihaila[a], Sigan L. Hartley[a], Annie D. Cohen[b], Dana L. Tudorascu[b], Peter D. Bulova[b], Brian J. Lopresti[b], Rameshwari V. Tumuluru[b], Dhanabalan Murali[a], Chester A. Mathis[b], Todd E. Barnhart[a], Charles K. Stone[a], Julie C. Price[b], Darlynne A. Devenny[c], Marsha R. Mailick[a], William E. Klunk[b], Sterling C. Johnson[a], Bradley T. Christian[a]

[a]*University of Wisconsin-Madison, Madison, WI, USA*
[b]*University of Pittsburgh, Pittsburgh, PA, USA*
[c]*New York State Institute for Basic Research in Developmental Disabilities, Albany, NY, USA*

Abstract

Introduction: Down syndrome (DS) arises from a triplication of chromosome 21, causing overproduction of the amyloid precursor protein and predisposes individuals to early Alzheimer's disease (AD).
Methods: Fifty-two nondemented adults with DS underwent two cycles of carbon 11-labeled Pittsburgh compound B ([^{11}C]PiB) and T1 weighted magnetic resonance imaging (MRI) scans 3.0 ± 0.6 years apart. Standard uptake value ratio (SUVR) images (50–70 minutes; cerebellar gray matter [GM]) and GM volumes were analyzed in standardized space (Montreal Neurological Institute space).
Results: 85% of PiB(−) subjects remained PiB(−), whereas 15% converted to PiB(+), predominantly in the striatum. None reverted from PiB(+) to PiB(−). Increases in SUVR were distributed globally, but there were no decreases in GM volume. The PiB positivity groups differed in the percent rate of change in SUVR [PiB(−): 0.5%/year, PiB converters: 4.9%/year, and PiB(+): 3.7%/year], but not in GM volume.
Discussion: Despite the characteristic striatum-first pattern, the global rate of amyloid accumulation differs by pre-existing amyloid burden and precedes atrophy or dementia in the DS population, similar to general AD progression.

Keywords: Down syndrome; Alzheimer's disease; Longitudinal; Amyloid PET; PiB

1. Introduction

Down syndrome (DS) is the most common genetic developmental disability (approximately 14.5 in every 10,000 live births [1]), and among other things, the triplicate copy of chromosome 21 leads to higher levels of amyloid precursor protein (APP) mRNA in DS brains compared with healthy controls [2]. In postmortem studies, elevated amyloid burden is apparent in adults with DS as early as their 20s and is nearly ubiquitous by their 40s in the same chemical form observed in Alzheimer's disease (AD) postmortem studies in the general population [3–5]. The combined effects of advances in medical procedures, better standard of care, and increased resource availability have led to a dramatic increase in life

*Corresponding author. Tel.: +1-608-890-2959; Fax: +1-608-262-9440.
E-mail address: plao@wisc.edu

http://dx.doi.org/10.1016/j.dadm.2017.05.001

expectancy, which is currently in the 60s, compared to approximately 9 years in the early 20th century [6].

Specific localization and sufficient density of amyloid-β plaques, often regarded as a consequence of reduced clearance of amyloid-β, are a neuropathologic hallmark of AD [7]. Thal staging of amyloid-β plaques in the general population suggests a hierarchical pattern with five phases. Nondemented cases may exhibit phases 1 through 3 in which phase 1 begins in the neocortex, phase 2 spreads to the allocortex, and phase 3 includes the diencephalic nuclei, striatum, and cholinergic nuclei of basal forebrain. Proven AD cases typically exhibit phases 3 through 5, where phase 4 involves several brainstem nuclei and phase 5 includes the cerebellum [8].

In <1% of all AD cases, there is a deterministic genetic predisposition to overexpression of amyloid-β and an early age of onset for dementia (<65 years) [9]. Autosomal dominant AD (ADAD) results from genetic mutations in APP (chromosome 21; 10–15% of ADAD cases), presenilin-1 (PSEN1; chromosome 14; 18%–50%), or presenilin-2 (PSEN2; chromosome 1; <5%) [10]. An interesting finding in individuals with ADAD is the striatum-dominant pattern of amyloid accumulation, regardless of mutation type [11,12]. In our previous cross-sectional study in the nondemented DS population, patterns of carbon 11-labeled Pittsburgh compound B ([^{11}C]PiB) binding demonstrated the elevated striatal binding in the absence of elevated neocortical binding [13]. These data suggest that a striatum-dominant pattern of amyloid-β plaque deposition in ADAD and DS may be a result of amyloid overproduction, consistent with other work [12–16].

Amyloid-β plaque accumulation precedes dementia, but the causal relationship is still unknown, as some cases never develop dementia despite the presence of plaques. In the DS population, the prevalence of dementia increases rapidly after the age of 30 years. It is estimated to be as high as 33% among individuals with DS aged 30 to 39 years, 55% among those aged 40 to 59 years, and 77% for individuals above the age of 60 years [17]. By comparison, the prevalence of dementia in the general population is estimated as 4% below 65 years, 15% between 65 and 74 years, 43% between 75 and 84 years, and 38% over the age of 85 years [18].

A comparison of DS adults with age-matched controls demonstrated a distinct pattern of gray matter (GM) reductions in hippocampus and adjacent medial temporal lobe that were independent of age and most likely reflect the abnormal brain morphology resulting from developmental disability [19]. In addition, others have suggested that age-related reductions in overall brain and GM volumes are not present until the onset of dementia [20]. GM reductions in allocortex and association neocortex in the nondemented DS population have been demonstrated using voxel-based morphometry, suggesting neuronal loss during the AD pathophysiologic process [21].

Knowledge of the disease course would inform future studies and therapeutic trials for which the DS population is a prime candidate. Moreover, findings regarding the natural history of amyloid-β accumulation and GM atrophy in the nondemented DS population may be generalizable to the predementia phase of any AD case. This study aims to identify the direction, magnitude, and regional distribution of changes in amyloid burden and GM volume in nondemented adults with DS.

2. Methods

2.1. Participants

The complete cohort (N = 81) was confirmed to be trisomic for chromosome 21 using genetic testing and recruited from a number of programs serving adults with DS and developmental disabilities (e.g., mailings to disability programs, fliers in DS clinics, research registries) located within 3 to 5 hours of the two performance sites (Waisman Center, University of Wisconsin-Madison; University of Pittsburgh Medical Center). Inclusion criteria included receptive language ≥3 years. Exclusion criteria included having a prior diagnosis of dementia, conditions that might contraindicate magnetic resonance imaging (MRI) (e.g., claustrophobia, metal in the body), and having a medical or psychiatric condition that impaired cognitive functioning.

Participants were assessed for dementia using the Down syndrome Dementia Scale (DSDS). Three individuals from the complete cohort received a cognitive cutoff score (CCS) >3 and were removed from analyses (N = 81 − 3 = 78). One individual had a CCS of 3 at entry but was included based on lower early and middle tally score on the DSDS, suggesting dementia was not present [22].

Out of the 78 nondemented participants, 52 (30–50 years old) completed two cycles of imaging and neuropsychologic evaluation (3.0 ± 0.6 years apart). Demographic information for the study cohort is summarized in Table 1. *APOE* ε4 allele information was obtained by genetic testing. The remaining subjects with only one cycle of data will be transitioned to a newly National Institutes of Health–funded biomarker study, Neurodegeneration in Aging Down Syndrome.

2.2. MRI acquisition

T1 weighted MRIs were acquired on a 3.0T GE SIGNA 750 (University of Wisconsin-Madison) or a 3.0T Siemens Magnetom Trio (University of Pittsburgh Medical Center). The SIGNA 750 acquisition used a high-resolution volumetric-spoiled gradient sequence (inversion time/echo time/repetition time = 450/3.2/8.2 ms, flip angle = 12°, slice thickness = 1 mm no gap, and matrix size = 256 × 256 × 156), whereas the Magnetom Trio acquisition used a magnetization-prepared rapid acquisition gradient echo sequence (inversion time/echo time/repetition time = 900/2.98/2300 ms, flip angle = 9°, slice thickness = 1.2 mm, matrix size = 160 × 240 × 256).

2.3. Positron emission tomography acquisition

On-site chemical synthesis of [^{11}C]PiB yielded high specific activity (≥2 mCi/nmol). Up to 15 mCi of [^{11}C]PiB was delivered intravenously via bolus injection (over 20–30 seconds) into the antecubital vein. Positron emission tomography

Table 1
Population demographics

Demographic information	Study cohort $N = 52$	PiB(−) $N = 35$	PiB converter $N = 6$	PiB(+) $N = 11$
Age at cycle 1 [years]*†	37.3 ± 6.6	34.8 ± 5.8	40.5 ± 5.8	43.5 ± 4.6
Time between cycles [years]*‡	3.0 ± 0.6	2.8 ± 0.5	3.9 ± 0.4	2.9 ± 0.5
Sex (M/F, %)	46.2/53.8	45.7/54.3	16.7/83.3	63.6/36.4
APOE ε4 positivity (noncarrier/carrier, %)	90.2/9.8	88.2/11.8	100/0	90.9/9.1
Standardized PPVT score at cycle 1	56.6 ± 17.2	57.1 ± 18.9	57.7 ± 13.3	54.5 ± 13.9
ITV at cycle 1 (mm^3)†	1,667,038 ± 106,666	1,687,847 ± 106,771	1,652,333 ± 66,696	1,608,851 ± 108,042

Abbreviations: ITV, intracranial total volume; F, female; M, male; PiB, Pittsburgh compound B; PPVT, Peabody Picture Vocabulary Test.

NOTE. An analysis of variance was used to find group differences in continuous variables, whereas a Pearson χ^2 test was used to find group differences in categorical variables. The PPVT score presented here is the standardized score, as opposed to the age equivalent score used in the analysis. This was done for an easier comparison to IQ.

*Significant difference between PiB(−) and PiB converter groups.

†Significant difference between PiB(−) and PiB(+) groups.

‡Significant difference between PiB converter and PiB(+) groups.

(PET) data were acquired on Siemens ECAT EXACT HR + PET scanners at both sites, and a $^{68}Ge/^{68}Ga$ transmission scan was acquired for 6 to 10 minutes to correct for the attenuation of annihilation radiation. Dynamic PET data (40–70 minutes postinjection, 6 × 5 minutes frames) were reconstructed using a filtered back-projection algorithm (direct inverse Fourier transform) and were corrected for detector dead time, scanner normalization, scatter, and radioactive decay.

2.4. Image processing

Preprocessing was performed in AIR, version 3.0 [23]. Dynamic PET data were corrected for interframe motion and averaged over 50 to 70 minutes postinjection. Parametric standard uptake value ratio (SUVR) images were generated from a cerebellar GM region of interest (ROI) and coregistered to skull-stripped, AC-PC–aligned T1wMRIs in native space.

Nonlinear spatial normalization was performed in a two-pass procedure for cycle 1 and cycle 2 images independently to reduce registration bias. In the first pass, the T1wMRIs were normalized to Montreal Neurological Institute space using the T1wMRI template provided in Statistical Parametric Mapping (toolbox in MATLAB) (www.fil.ion.ac.uk/spm/software/). The transformation matrix was applied to the coregistered SUVR images to bring them into MNI space. To allow the inclusion of subjects with excessive motion artifacts in their T1wMRIs, a subset of the normalized SUVR images were averaged and smoothed (8-mm gaussian) to create a DS-specific PET PiB template. In the second pass, the native space SUVR images were normalized to the DS-specific PET template, and the transformation matrix was applied to the coregistered T1wMRI. The normalized images were visually inspected in cine mode and qualitatively assessed on cortical outline and striatal placement. Small improvements in spatial normalization via the DS-specific PET template were observed in subjects with motion in their T1wMRI. No images were removed because of poor spatial normalization via the DS-specific PET template.

Tissue type segmentation was similarly performed in a two-pass procedure, creating DS-specific GM, white matter (WM), and cerebrospinal fluid (CSF) prior probability maps. In the first pass, the spatially normalized T1wMRIs were segmented using the GM, WM, and CSF prior probability maps in MNI space provided in SPM. A subset of segmented images were averaged and smoothed (8-mm gaussian) to create DS-specific tissue type prior probability maps. In the second pass, the normalized T1wMRIs were segmented using the DS specific tissue type prior probability maps, similar to methods often used for atypical populations [21]. The segmented images were visually inspected for reasonable tissue-type segmentation. The intracranial total volume (ITV) was calculated from GM, WM, and CSF segmented images.

ROIs were defined in MNI space from the Talairach-Daemon database, provided in the Wake Forest University PickAtlas toolbox in SPM. The investigated ROIs included the anterior cingulate, frontal cortex, parietal cortex, precuneus, striatum, and temporal cortex. The binary masks were dilated (4-mm gaussian smoothing and thresholding at 0.3) to account for intersubject variability in brain morphology that may have persisted after spatial normalization. ROI masks were closely inspected to ensure proper coverage for each region on each subject.

2.5. PiB positivity

ROI-specific PiB positivity thresholds were determined by sparse k-means clustering with resampling using a previously described process [24], applied to non–atrophy-corrected data from the complete cohort [13,25]. A subject was classified as PiB(+) if at least one ROI exceeded its threshold (anterior cingulate, 1.59; frontal cortex, 1.48; parietal cortex, 1.51; precuneus, 1.64; striatum, 1.45; and temporal cortex, 1.38). PiB positivity groups will be referred to as PiB(−) (PiB(−) at both cycles), PiB converters (PiB(−) at cycle 1 and PiB(+) at cycle 2), or PiB(+) (PiB(+) at both cycles).

2.6. Cognitive function

Participants completed a comprehensive neuropsychological evaluation assessing a range of domains, including

Table 2
Descriptive statistics [mean (standard deviation)] for PiB SUVR and GM volume for each ROI, as well as PPVT score, at cycle 1 and cycle 2, stratified by PiB positivity groups

	Study cohort $N = 52$	PiB(−) $N = 35$	PiB converter $N = 6$	PiB(+) $N = 11$
Region of interest	PiB SUVR at cycle 1; cycle 2			
Anterior cingulate	1.27 (0.26); 1.34 (0.32)*	1.16 (0.10); 1.17 (0.12)	1.20 (0.12); 1.42 (0.07)*	1.67 (0.29); 1.83 (0.31)*
Frontal cortex	1.17 (0.26); 1.24 (0.33)*	1.06 (0.10); 1.07 (0.11)	1.09 (0.09); 1.31 (0.05)*	1.57 (0.29); 1.76 (0.34)*
Parietal cortex	1.19 (0.27); 1.27 (0.34)*	1.07 (0.10); 1.09 (0.11)	1.12 (0.11); 1.34 (0.15)	1.62 (0.27); 1.80 (0.34)*
Precuneus	1.26 (0.28); 1.34 (0.35)*	1.14 (0.09); 1.15 (0.11)	1.17 (0.10); 1.43 (0.14)*	1.69 (0.30); 1.88 (0.35)*
Striatum	1.31 (0.37); 1.41 (0.43)*	1.13 (0.10); 1.16 (0.12)	1.27 (0.15); 1.58 (0.19)*	1.91 (0.35); 2.11 (0.36)*
Temporal cortex	1.18 (0.20); 1.23 (0.27)*	1.09 (0.08); 1.09 (0.10)	1.14 (0.09); 1.25 (0.13)	1.49 (0.21); 1.63 (0.27)*
	GM volume at cycle 1; cycle 2 (mm^3)			
Anterior cingulate	6327 (1082); 6462 (1034)	6312 (1120); 6642 (1024)	6376 (1259); 6172 (1030)	6347 (954); 6052 (1005)
Frontal cortex	17,989 (4012); 18,073 (3744)	17,866 (4220); 18,555 (3892)	17,607 (3500); 17,234 (3647)	18,588 (3857); 16,997 (3293)
Parietal cortex	15,745 (2733); 16,006 (2463)	15,660 (3154); 16,490 (2590)*	15,780 (1134); 14,887 (1779)	16,000 (1880); 15,075 (2004)*
Precuneus	18,608 (2459); 18,680 (2672)	18,795 (2752); 19,357 (2638)	18,346 (1414); 17,480 (1999)	18,159 (1928); 17,180 (2413)
Striatum	12,656 (1861); 12,638 (1991)	12,616 (1869); 12,785 (2027)	12,078 (1702); 11,483 (1722)	13,098 (1978); 12,798 (1964)
Temporal cortex	7206 (833); 7199 (743)	7259 (895); 7384 (712)	7108 (793); 7000 (740)	7088 (684); 6721 (653)
	PPVT score at cycle 1; cycle 2 (years)			
Global measure	98.3 (41.3); 96.2 (39.9)	100.9 (46.2); 100.9 (41.8)	97.8 (28.1); 89.0 (35.5)	90.3 (30.9); 84.8 (36.3)

Abbreviations: GM, gray matter; PiB, Pittsburgh compound B; PPVT, Peabody Picture Vocabulary Test; ROI, region of interest; SUVR, standard uptake value ratio.

*A significant unadjusted mean difference between cycle 1 and cycle 2.

verbal learning and memory, visual memory, attention/processing speed, executive/working memory, visuoconstruction, and language. Current analysis is limited to the Peabody Picture Vocabulary Test (PPVT) (4th Edition), which is a measure of receptive language that correlates strongly with IQ scores. The PPVT score was calculated as an age equivalent and is often used as a surrogate measure of overall cognitive performance in the DS population [21].

2.7. Statistical analysis

Descriptive statistics (mean and standard deviation) were calculated for PiB SUVR, GM volume, and PPVT (Table 2). All analyses were performed in IBM SPSS Statistics 21.0, test statistics were tested with a two-sided test, and considered significant after a Bonferroni correction for multiple comparisons ($\alpha = 0.05/6$ ROIs $= 0.008$). Tests were performed in the study cohort ($N = 52$), and sensitivity analyses were performed in the PiB(−) ($N = 35$), the PiB converter ($N = 6$), and the PiB(+) ($N = 11$) groups, individually.

Paired *t*-tests were used to assess the changes in PiB SUVR, GM volume, or PPVT score from cycle 1 to cycle 2. Percent rates of change in PiB SUVR, GM volume, or PPVT [(cycle 2 − cycle 1)/(cycle 1 × 100)/time between cycles] were tested for differences between PiB positivity groups in one-way analyses of variance. Pearson pairwise correlation coefficients were computed for the values of PiB SUVR, GM volume, and PPVT, as well as the percent rates of change in each.

Covariates of interest (e.g., time between cycles, age, sex, *APOE* ε4 positivity, and either PiB SUVR, GM volume, or PPVT score depending on the outcome measure) were investigated individually. Adjustments for PiB SUVR or GM volume were limited to local effects. For instance, analysis of the anterior cingulate was kept separate from that of the frontal cortex.

3. Results

3.1. Change in PiB SUVR, GM volume, and PPVT score

The 52 nondemented adults with DS demonstrated no significant change in SUV in cerebellar GM between cycles (cycle 2 − cycle 1 [95% confidence interval]: −0.03 [−0.06, 0.01]), supporting its suitability as a reference region. Increases in PiB SUVR between cycles were distributed across the neocortex and striatum, shown in Fig. 1. Notably, there was a significant increase in the mean SUVR in all investigated ROIs (Table 2), which survived separate adjustment for all covariates except *APOE* ε4 positivity in the temporal cortex. There were no significant changes in GM volume or PPVT score (Table 2), with or without adjustment for covariates.

Results from the correlation analyses are presented in Supplementary Table 1. There was a significant negative correlation between %GM/year and age in the precuneus, that is, older participants had more negative percent rates of change. There was also a significant negative correlation between %GM/year and PiB SUVR in the parietal cortex and precuneus. The %GM/year in the striatum was positively associated with the %ITV/year, that is, the volume of the striatum changed proportionally with the intracranial total volume. The %SUVR/year or %PPVT/year was not significantly correlated with any covariates.

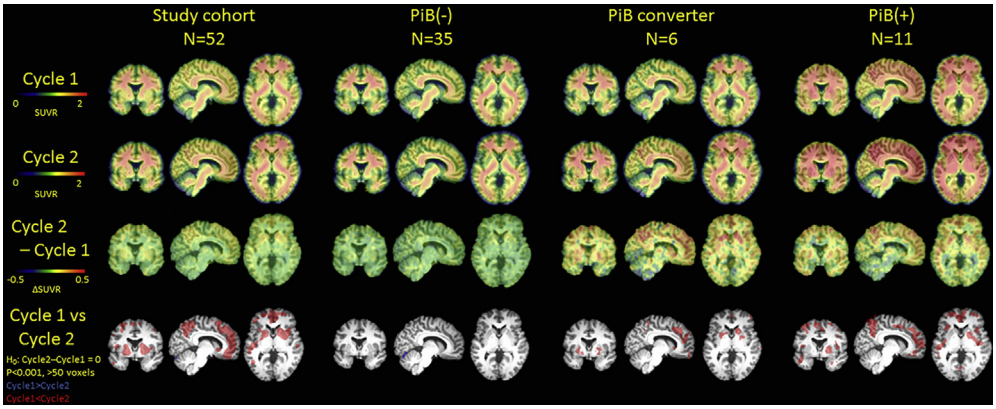

Fig. 1. Average images of PiB SUVR at cycle 1 and cycle 2, as well as the difference image between cycles and parametric *t*-maps indicating clusters of significant differences between cycles ($P < .001$, >50 voxels). Abbreviations: PiB, Pittsburgh compound B; SUVR, standard uptake value ratio.

3.2. PiB positivity

Out of the 41 PiB(−) subjects at cycle 1, 35 of 41 (85%) subjects remained PiB(−) (Fig. 2; blue lines). The average %SUVR/year was 0.5 ± 0.3%/year across all ROIs. However, the PiB(−) group contained a few subjects with increases in PiB SUVR (Fig. 2), indicating heterogeneity within the PiB(−) group. In addition, 6 of 41 (15%) subjects converted to PiB(+), and the majority (4/6, 67%) crossed the threshold in the striatum only (Fig. 2; green lines), which indicates that the striatum is typically the first region to begin amyloid accumulation. There was a 4.9 ± 1.4%/year increase across all ROIs, despite most subjects being considered a converter only in the striatum. Importantly, 11 of 11 (100%) subjects remained PiB(+), indicating that there were no subjects who showed evidence of reversible amyloid accumulation. PiB(+) subjects (Fig. 2; red lines) also tended to show a 3.7 ± 0.4%/year increase across all ROIs.

3.3. Differential changes in PiB SUVR by PiB positivity groups

The PiB(−) group demonstrated no significant changes in PiB SUVR between cycles in any ROI (Table 2), with or without adjustment for covariates. The PiB converter group demonstrated significant increases in PiB SUVR in the anterior cingulate, frontal cortex, precuneus, and striatum (Table 2). The increase in the anterior cingulate did not survive adjustment for sex. The increase in the precuneus did not survive adjustment for age, sex, *APOE* ε4 positivity, GM volume, or PPVT. The PiB(+) group demonstrated significant increases in PiB SUVR in all ROIs (Table 2), which survived adjustment for each covariate.

There were significant group differences in %SUVR/year between the PiB(−) and PiB converter groups [PiB converter > PiB(−)] in all ROIs, except the temporal cortex (Table 3). Adjustment for age in the striatum resulted in a loss of significance. Adjustment for age in the temporal

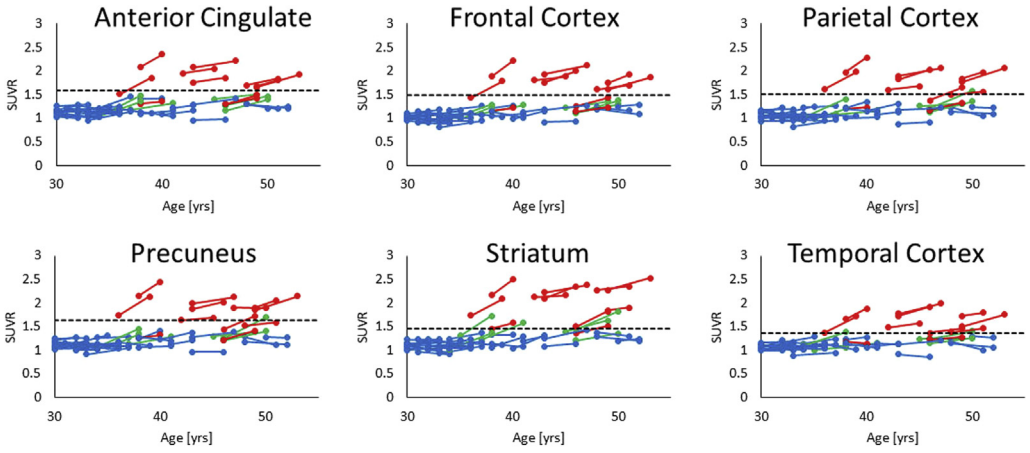

Fig. 2. Longitudinal plots of mean PiB SUVR against age with the PiB positivity thresholds in each ROI shown as the dotted line. Each line represents a non-demented adult with DS. The PiB(−) group ($N = 35$) is shown in blue, the PiB converter group ($N = 6$) is shown in green, and the PiB(+) group ($N = 11$) is shown in red. Abbreviations: PiB, Pittsburgh compound B; ROI, region of interest; SUVR, standard uptake value ratio.

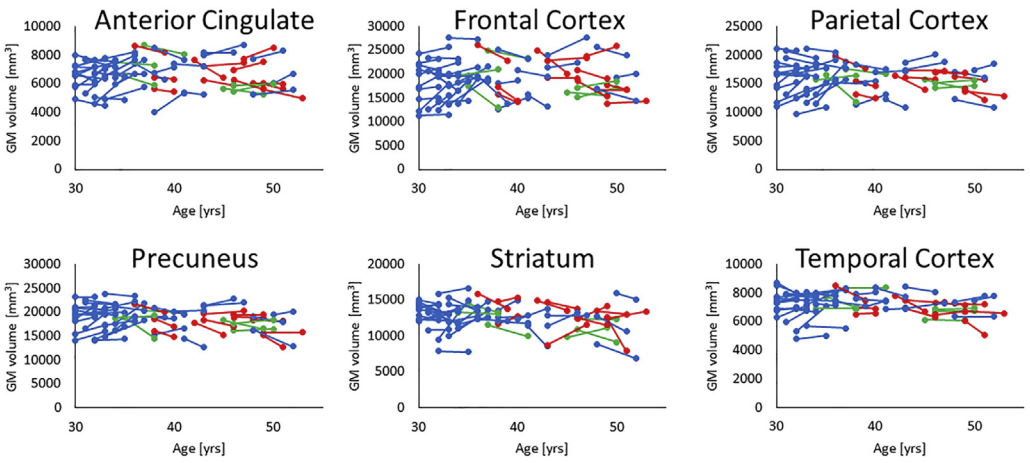

Fig. 3. Longitudinal plots of mean GM volume against age. Each line represents a nondemented adult with DS. The PiB(−) group ($N = 35$) is shown in blue, the PiB converter group ($N = 6$) is shown in green, and the PiB(+) group ($N = 11$) is shown in red. Abbreviations: PiB, Pittsburgh compound B; SUVR, standard uptake value ratio.

cortex resulted in a significant group difference [PiB converter > PiB(−)] that was not apparent without adjustment. There were also significant group differences in % SUVR/year between the PiB(−) and PiB(+) groups [PiB(+) > PiB(−)] in all ROIs (Table 3), which survived adjustment for each covariate. There were no significant group differences in %SUVR/year between the PiB converter and PiB(+) groups, with or without adjustment for any covariates (Table 3). In addition, there were no significant correlations between %SUVR/year and any covariates within any of the PiB positivity groups (Supplementary Table 1).

3.4. Differential changes in GM volume by PiB positivity groups

In the PiB(−) group, there was a significant increase in GM volume between cycles in the parietal cortex (Table 2), which did not survive adjustment for time between cycles, sex, *APOE* ε4 positivity, or PPVT. In the PiB converter group, there were no significant changes in GM volume in any ROI (Table 2), with or without adjustment for covariates. In the PiB(+) group, there was a significant decrease in the parietal cortex (Table 2). A significant decrease in the precuneus became apparent when adjusting for the time between cycles.

Table 3
Summary of the mean percent change in PiB SUVR, GM volume, and PPVT score per year in each ROI for each PiB positivity group

	PiB(−) $N = 35$	PiB converter $N = 6$	PiB(+) $N = 11$
Region of interest	Percent change in SUVR per year		
Anterior cingulate*†	0.2%, [−0.6, 1.1]	4.8%, [2.2, 7.5]	3.5%, [2.3, 4.8]
Frontal cortex*†	0.4%, [−0.4, 1.3]	5.3%, [3.4, 7.1]	4.2%, [2.7, 5.8]
Parietal cortex*†	0.6%, [−0.3, 1.4]	5.1%, [1.9, 8.3]	4.0%, [2.5, 5.5]
Precuneus*†	0.5%, [−0.4, 1.3]	5.6%, [2.6, 8.6]	3.9%, [2.5, 5.4]
Striatum*†	0.9%, [−0.1, 1.9]	6.4%, [4.0, 8.9]	3.7%, [2.1, 5.3]
Temporal cortex†	0.1%, [−0.7, 0.9]	2.4%, [0.4, 4.4]	3.1%, [1.3, 4.9]
	Percent change in GM per year		
Anterior cingulate	2.2%, [0.6, 3.8]	−0.8%, [−2.9, 1.4]	−1.7%, [−3.2, −0.1]
Frontal cortex	2.1%, [−0.1, 4.3]	−0.7%, [−4.9, 3.6]	−3.1%, [−5.3, −0.8]
Parietal cortex†	2.4%, [0.8, 4.1]	−1.6%, [−5.4, 2.1]	−2.2%, [−3.5, −0.9]
Precuneus†	1.3%, [0.1, 2.4]	−1.4%, [−4.6, 1.8]	−2.2%, [−3.9, −0.6]
Striatum	0.6%, [−1.2, 2.4]	−1.1%, [−4.2, 2.0]	−0.6%, [−4.8, 3.7]
Temporal cortex	0.8%, [−0.1, 1.7]	−0.4%, [−1.7, 0.8]	−1.8%, [−3.5, −0.2]
	Percent change in PPVT per year		
Global measure	2.8%, [−2.3, 7.9]	−2.6%, [−8.7, 3.4]	−2.9%, [−9.2, 3.4]

Abbreviations: GM, gray matter; PiB, Pittsburgh compound B; PPVT, Peabody Picture Vocabulary Test; ROI, region of interest; SUVR, standard uptake value ratio.
NOTE. There were no significant differences between the PiB converter and PiB(+) groups.
*A significant difference between the PiB(−) and PiB converter groups.
†A significant difference between the PiB(−) and PiB(+) groups.

Longitudinal change in GM volume is shown in Fig. 3 by PiB positivity group.

There were significant group differences in %GM/year between the PiB(−) and PiB(+) groups [PiB(−) > PiB(+)] in the parietal cortex and precuneus, which did not survive adjustment for age (Table 3). In addition, there was a significant positive correlation between %GM/year in the striatum and %ITV/year in the PiB(+) group (Supplementary Table 1).

3.5. Differential changes in PPVT score by PiB positivity groups

There were no significant changes in PPVT score in any of the PiB positivity groups (Table 2), but there was a significant decrease in PPVT between cycles after adjusting for %GM/year in the temporal cortex within the PiB(+) group.

There were no group differences in %PPVT/year (Table 3), but there was a nonsignificant trend of larger decreases in %PPVT/year across the PiB positivity groups [PiB(−) > PiB converter > PiB(+)]. There was a positive correlation between %PPVT/year and %ITV/year in the PiB(+) group (Supplementary Table 1).

4. Discussion

In a nondemented population of adults with DS, there was an increase in amyloid that was distributed across the neocortex and striatum over 3.0 ± 0.6 years. The rate of conversion from PiB(−) to PiB(+) was 5%/year, which can be compared to that reported in a study of cognitively normal adults (aged 45–86 years) in which there was a 3.1%/year rate of conversion to amyloid positivity [26]. While many of the correlation coefficients between amyloid accumulation and covariates were weak and only a few were significant, the correlation coefficients tended to be in the expected direction (Supplementary Table 1). For instance, the direction of the correlation coefficients indicated that older adults, adults with an elevated amyloid burden, and adults with a low PPVT tend to accumulate amyloid at a faster rate.

There have been studies indicating amyloid seeding as a mechanism of amyloidogenesis. For instance, APP-transgenic mice studies have demonstrated amyloid deposition following the infusion of AD-brain homogenates and no amyloid deposition following the infusion of healthy brain homogenates [27]. In our data, there was a 10-fold increase in amyloid deposition between PiB positivity groups [0.5%/year increase in SUVR for PiB(−) and 3.7%/year increase in SUVR for PiB(+)] suggesting that pre-existing amyloid burden accelerates amyloid deposition. Similarly, a study found a 0.5% increase per year in elderly healthy controls (aged 73.1 ± 7.5 years) and a 3.4% increase per year in subjects with AD (aged 71.7 ± 8.9 years), where healthy controls would have significantly less amyloid deposition compared with AD subjects [28]. Other studies have shown no significant increases in PiB SUVR in subjects with later stage AD, indicating that there is a plateau of amyloid burden during the period of cognitive decline [29]. However, this plateau in amyloid accumulation was not observed in the PiB(+) group in these adults with DS.

There were no significant changes in GM volume across the whole cohort in any of the investigated ROIs before the onset of dementia. There was an increase in GM volume in the PiB(−) group; however, it did not survive adjustment for age. On average, the differences in %GM volume/year between the PiB positivity groups suggest that GM atrophy is only apparent in the parietal cortex and precuneus, given an elevated amyloid burden. GM atrophy in the striatum was associated with a decrease in the ITV, meaning that it was proportional to the total brain volume rather than accelerated by the striatum-dominant amyloid deposition. The study cohort remained nondemented (CCS < 3) at follow-up, and there was a nonsignificant negative trend in the rate of change in PPVT that followed the trend in GM atrophy. A previous study has reported an association between amyloid positivity and greater brain atrophy, as well as between amyloid positivity and greater cognitive decline, but results were driven by those with mild cognitive impairment [30].

Neuropathologic studies demonstrate that amyloid plaques in the DS population share a common protein core with those in the general population [5]. Furthermore, neuropathologic and longitudinal imaging studies in ADAD showed that the composition of amyloid plaques and the temporal progression of AD neuropathologic changes were consistent with that observed in the general population, respectively [9,31]. Results from populations that experience an overproduction of amyloid (e.g., DS and ADAD) to populations that experience a reduced clearance of amyloid (e.g., general population) may be generalizable because all populations accumulate the same amyloid aggregates and experience the same overall temporal progression of AD in which amyloid accumulation precedes neurodegeneration and dementia [31,32].

While this study represents the largest longitudinal study of amyloid deposition and GM atrophy in the nondemented DS population, there are some limitations. Accumulation of amyloid pathology and GM atrophy in DS is superimposed on an already affected neural substrate with pre-existing developmental abnormalities, including defects in neurogenesis and synaptogenesis, as well as reduced volumes of specific brain regions. But just as neuropathologic changes must be assessed in the context of the individual's lifelong cognitive function, longitudinal studies in which subjects serve as their own control could potentially disambiguate changes in amyloid burden and GM volume from the DS phenotype.

Future work includes the continuation of this work as a part of the recently initiated multisite Neurodegeneration in Aging Down Syndrome study, which incorporates additional imaging, biofluid, and genetic biomarkers. Investigation of GM atrophy will be extended to multispectral tissue-type segmentation, and possible WM hyperintensities will be evaluated using T2 fluid attenuation inversion recovery images. Furthermore, investigation of cognitive decline is currently being extended to more specific cognitive domains such as episodic memory (Hartley 2017, under review).

Acknowledgments

The authors would like to thank the psychologists, project managers (Travis Doran, Renee Makuch, Cathleen Wolfe, David Maloney, and Sarah Clayton), scientists (Jeffrey James), and technologists (Barbara Mueller) at the University of Wisconsin-Madison and University of Pittsburgh-Medical Center and their Alzheimer's Disease Research Centers who make this research possible. We would also like to thank the adults with Down syndrome and their families for their time and commitment to further discovery and understanding into the causes of Alzheimer's disease.
The research is funded by the National Institute of Aging (R01AG031110 to B.L.H. and B.T.C.; U01AG051406 to B.L.H., W.E.K., and B.T.C.) and the National Institute on Child Health and Human Development (P30 HD03352 to M.R.M.).

Supplementary data

Supplementary data related to this article can be found at http://dx.doi.org/10.1016/j.dadm.2017.05.001.

RESEARCH IN CONTEXT

1. Systematic review: The authors performed a literature search covering Down syndrome (DS), Alzheimer's disease (AD), and longitudinal amyloid-β and gray matter imaging. There are several longitudinal amyloid positron emission tomography (PET) studies in late-onset sporadic AD (context of reduced amyloid clearance), but few in early-onset autosomal dominant AD or AD in DS (context of amyloid overproduction).
2. Interpretation: Our findings demonstrate an increase in amyloid burden that does not reach a plateau in the nondemented DS population. The rate of amyloid accumulation is associated with the existing amyloid burden. Increases in amyloid precede the changes in gray matter or the onset of dementia, which suggests consistency of the AD pathophysiologic process in the DS and the general population.
3. Future directions: [^{18}F]fluorodeoxyglucose and [^{18}F] AV-1451 PET scans will be acquired in addition to the carbon 11-labeled Pittsburgh compound B PET scans for a more comprehensive understanding of AD pathophysiologic process in the nondemented DS population. Furthermore, several other magnetic resonance imaging sequences will be obtained (T2 fluid attenuated inversion recovery, diffusion tensor imaging, arterial spin labeling, and resting-state functional magnetic resonance imaging).

References

[1] Parker SE, Mai CT, Canfield MA, Rickard R, Wang Y, Meyer RE, et al. Updated national birth prevalence estimates for selected birth defects in the United States, 2004–2006. Birth Defects Res A Clin Mol Teratol 2010;88:1008–16.
[2] Oyama G, Cairns NJ, Shimada H, Oyama R, Titani K, Ihara Y. Down's syndrome: up-regulation of β-amyloid protein precursor and τ mRNAs and their defective coordination. J Neurochem 1994;62:1062–6.
[3] Wisniewski KE, Wisniewski HM, Wen GY. Occurrence of neuropathological changes and dementia of Alzheimer's disease in Down's syndrome. Ann Neurol 1985;17:278–82.
[4] Mann DM, Esiri MM. The pattern of acquisition of plaques and tangles in the brains of patients under 50 years of age with Down's syndrome. J Neurol Sci 1989;89:169–79.
[5] Masters CL, Simms G, Weinman NA, Multhaup G, McDonald BL, Beyreuther K. Amyloid plaque core protein in Alzheimer disease and Down syndrome. Proc Natl Acad Sci U S A 1985;82:4245–9.
[6] Zigman WB, Devenny DA, Krinsky-McHale SJ, Jenkins EC, Urv TK, Wegiel J, et al. Alzheimer's disease in adults with Down syndrome. Int Rev Res Ment Retard 2008;36:103–45.
[7] Hyman BT, Phelps CH, Beach TG, Bigio EH, Cairns NJ, Carrillo MC, et al. National Institute on Aging-Alzheimer's Association guidelines for the neuropathologic assessment of Alzheimer's disease. Alzheimers Dement 2012;8:1–13.
[8] Thal DR, Rüb U, Orantes M, Braak H. Phases of Aβ-deposition in the human brain and its relevance for the development of AD. Neurology 2002;58:1791–800.
[9] Bateman RJ, Aisen PS, De Strooper B, Fox NC, Lemere CA, Ringman JM, et al. Autosomal-dominant Alzheimer's disease: a review and proposal for the prevention of Alzheimer's disease. Alzheimers Res Ther 2011;3:1.
[10] Bekris LM, Yu C, Bird TD, Tsuang DW. Genetics of Alzheimer disease. J Geriatr Psychiatry Neurol 2010;23:213–27.
[11] Klunk WE, Price JC, Mathis CA, Tsopelas ND, Lopresti BJ, Ziolko SK, et al. Amyloid deposition begins in the striatum of presenilin-1 mutation carriers from two unrelated pedigrees. J Neurosci 2007;27:6174–84.
[12] Villemagne VL, Ataka S, Mizuno T, Brooks WS, Wada Y, Kondo M, et al. High striatal amyloid β-peptide deposition across different autosomal Alzheimer's disease mutation types. Arch Neurol 2009;66:1537–44.
[13] Lao PJ, Betthauser TJ, Hillmer AT, Price JC, Klunk WE, Mihaila I, et al. The effects of normal aging on amyloid-β deposition in nondemented adults with Down syndrome as imaged by carbon 11-labeled Pittsburgh compound B. Alzheimers Dement 2016;12:380–90.
[14] Annus T, Wilson LR, Hong YT, Acosta–Cabronero J, Fryer TD, Cardenas–Blanco A, et al. The pattern of amyloid accumulation in the brains of adults with Down syndrome. Alzheimers Dement 2016;12:538–45.
[15] Handen BL, Cohen AD, Channamalappa U, Bulova P, Cannon SA, Cohen WI, et al. Imaging brain amyloid in nondemented young adults with Down syndrome using Pittsburgh compound B. Alzheimers Dement 2012;8:496–501.
[16] Rafii MS, Wishnek H, Brewer JB, Donohue MC, Ness S, Mobley WC, et al. The Down syndrome biomarker initiative (DSBI) pilot: proof of concept for deep phenotyping of Alzheimer's disease biomarkers in Down syndrome. Front Behav Neurosci 2015;9:239.
[17] Head E, Lott IT, Patterson D, Doran E, Haier RJ. Possible compensatory events in adult Down syndrome brain prior to development of Alzheimer disease neuropathology: targets for nonpharmacological intervention. J Alzheimers Dis 2007;11:61–76.
[18] Hebert LE, Weuve J, Scherr PA, Evans DA. Alzheimer disease in the United States (2010–2050) estimated using the 2010 Census. Neurology 2013;80:1778–83.

[19] White NS, Alkire MT, Haier RJ. A voxel-based morphometric study of nondemented adults with Down syndrome. Neuroimage 2003; 20:393–403.
[20] Kesslak JP, Nagata SF, Lott I, Nalcioglu O. Magnetic resonance imaging analysis of age-related changes in the brains of individuals with Down's syndrome. Neurology 1994;44:1039–45.
[21] Teipel SJ, Alexander GE, Schapiro MB, Möller HJ, Rapoport SI, Hampel H. Age-related cortical grey matter reductions in nondemented Down's syndrome adults determined by MRI with voxel-based morphometry. Brain 2004;127:811–24.
[22] Gedye A. Dementia Scale for Down syndrome. Vancouver: Gedye Research and Consulting; 1995.
[23] Woods RP, Grafton ST, Holmes CJ. Automated image registration: I. General methods and intrasubject, intramodality validation. J Comput Assist Tomogr 1998;22:139–52.
[24] Cohen AD, Mowrey W, Weissfel LA, Aizenstein HJ, McDade E, Mountz JM, et al. Classification of amyloid-positivity in controls: comparison of visual read and quantitative approaches. Neuroimage 2013;71:207–15.
[25] Hartley SL, Handen BL, Devenny DA, Hardison R, Mihaila I, Price JC, et al. Cognitive functioning in relation to brain amyloid-β in healthy adults with Down syndrome. Brain 2014;137:1–8.
[26] Vlassenko AG, Mintun MA, Xiong C, Sheline YI, Goate AM, Benzinger TL, et al. Amyloid-beta plaque growth in cognitively normal adults: longitudinal [11C]Pittsburgh compound B data. Ann Neurol 2011;70:857–61.
[27] Kane MD, Lipinski WJ, Callahan MJ, Bian F, Durham RA, Schwarz RD, et al. Evidence for seeding of β-amyloid by intracerebral infusion of Alzheimer brain extracts in β-amyloid precursor protein-transgenic mice. J Neurosci 2000;20:3606–11.
[28] Villemagne VL, Pike KE, Chetelat G, Ellis KA, Mulligan RS, Bourgeat P, et al. Longitudinal assessment of Aβ and cognition in aging and Alzheimer's disease. Ann Neurol 2011;69:181–92.
[29] Engler H, Forsberg A, Almkvist O, Blomquist G, Larsson E, Savitcheva I, et al. Two-year follow-up of amyloid deposition in patients with Alzheimer's disease. Brain 2006;129:2856–66.
[30] Jack CR Jr, Wiste HJ, Weigand SD, Knopman DS, Lowe V, Vemuri P, et al. Amyloid-first and neurodegeneration-first profiles characterize incident amyloid PET positivity. Neurology 2013; 81:1732–40.
[31] Yau WW, Tudorascu DL, McDade EM, Ikonomovic S, James JA, Minhas D, et al. Longitudinal assessment of neuroimaging and clinical markers in autosomal dominant Alzheimer's disease: a prospective cohort study. Lancet Neurol 2015;14:804–13.
[32] Villemagne VL, Burnham S, Bourgeat P, Brown B, Ellis KA, Salvado O, et al. Amyloid β deposition, neurodegeneration, and cognitive decline in sporadic Alzheimer's disease: a prospective cohort study. Lancet Neurol 2013;12:357–67.